Nanohybrid Kaolinite-Based Materials Obtained from the Interlayer Grafting of 3-Aminopropyltriethoxysilane and Their Potential Use as Electrochemical Sensors

Ignas K. Tonlé,[†,‡] Thomas Diaco,[†] Emmanuel Ngameni,[§] and Christian Detellier*[,†]

Centre for Catalysis Research and Innovation and Department of Chemistry, University of Ottawa, 10 Marie Curie, Ottawa, Ontario K1N 6N5, Canada; Département de Chimie, Faculté des Sciences, Université de Dschang, B. P. 67 Dschang, Cameroun; and Laboratoire de Chimie Analytique, Faculté des Sciences, Université de Yaoundé 1, B. P. 812 Yaoundé, Cameroun

Received August 6, 2007. Revised Manuscript Received October 22, 2007

The grafting of 3-aminopropyltriethoxysilane (APTES) onto the internal aluminol groups of two kaolinite minerals from Georgia and from Cameroon was achieved by utilizing their corresponding dimethyl sulfoxide (DMSO) intercalation compounds as intermediates. The modified clays were characterized by powder X-ray diffraction, thermal gravimetric analysis coupled with mass spectrometry, Fourier transform infrared, and solid-state MAS NMR. These techniques demonstrated the effectiveness of the interlamellar grafting process. An expansion of the interlayer distance from 11.2 to 15.9–16.4 Å on going from the precursors to the nanohybrid materials was observed. The study of the thermal behavior of the organoclays showed the release under heating of grafted APTES fragments, typical of the decomposition products of carbon, hydrogen, and nitrogen bearing organic matter. The hydroxyl stretching vibration zone (3700–3600 cm^{-1}) of the starting clays and of the DMSO intercalated precursors was intensively perturbed in the final materials. New bands were observed, indicating strong interactions between APTES and the kaolinite interlayer surfaces. Solid-state ^{29}Si CP-MAS NMR spectra of silylated kaolinite showed T^2 and T^3 signals corresponding to the linkage of APTES moieties. This was confirmed by the relative intensities of the signals in the quantitative ^{13}C CP-MAS NMR spectra of the nanohybrid materials. Concomitant silylation and ethoxylation of the interlayer aluminol surface were obtained to give a mixed alkoxy–organosilyl kaolinite derivative. The silylation was roughly equally distributed between bidentate and tridentate fixations, with a minor amount of monodentate material. A remarkable feature of the new materials was their response to the $[Ru(CN)_6]^{4-}$ electrochemical probe in acidic medium when the functionalized clays were coated on a platinum electrode. This is due to the protonated amine groups that act as anion exchange sites. These preliminary results open the way to further development of kaolinite-based electrochemical sensors.

Introduction

Over the past decade, the development of nanohybrid materials based on the binding of organic and inorganic units at the molecular scale has attracted growing interest. A major appeal of such research activities is the building of advanced materials with well-controlled composition and properties, displaying attractive applications in the fields of environmental, catalysis, and material sciences.[1] In that context, clay materials play an important role as parent host structure for organic compounds, owing to their intrinsic properties such as chemical and thermal stability, ion exchange, and the presence on their interlayer surfaces of hydroxyl group active sites.[2]

As yet, smectites are the most used class of phyllosilicates for the elaboration of nanohybrid and nanocomposite materials due to their swelling properties, their high exchange capacity, and surface area. Most common methods used for their chemical modification include sol–gel process,[3] ion exchange of their inherent interlayer cations by quaternary alkylammonium,[4] photoactive cationic species[5] or polyhydroxometallic cations,[6] the intercalation of ionic biopolymers,[7] and the covalent grafting of organosilanes.[8] The latter method is of key importance since the linkage of organic components via covalent bonds enables a durable im-

* Corresponding author. E-mail: dete@uottawa.ca.
† University of Ottawa.
‡ Université de Dschang.
§ Université de Yaoundé 1.

(1) (a) *Functional Hybrid Materials*; Gómez-Romero, P., Sanchez, C., Eds.; Wiley-VCH: Weinheim, 2004. (b) Ruiz-Hitzky, E. *Chem. Rec.* **2003**, *3*, 88–100.
(2) (a) *Handbook of Clay Science, Developments in Clay Science 1*; Bergaya, F., Theng, B. K. G., Lagaly, G., Eds.; Elsevier: Amsterdam, 2006. (b) Lagaly, G.; Ogawa, M.; Dekany, I. Mineral Organic Interactions. In *Handbook of Clay Science, Developments in Clay Science, 1*; Bergaya, F., Theng, B. K. G., Lagaly, G., Eds.; Elsevier: Amsterdam, 2006;Chapter 7.3, pp 309–377.
(3) (a) da Fonseca, M. G.; Silva, C. R.; Airoldi, C. *Langmuir* **1999**, *15*, 5048–5055. (b) Letaief, S.; Ruiz-Hitzky, E. *Chem. Commun.* **2003**, *24*, 2996–2997.
(4) (a) Othmani-Assmann, H.; Benna-Zayani, M.; Geiger, S.; Fraisse, B.; Kbir-Ariguib, N.; Trabelsi-Ayadi, M.; Ghermani, N. E.; Grossiord, J. L *J. Phys. Chem. C* **2007**, *111*, 10869–10877. (b) Lee, S. Y.; Kim, S. J. *Clays Clay Miner.* **2002**, *50*, 435–445. (c) Choy, J. H.; Kwak, S. Y.; Han, Y. S.; Kim, B. W. *Mater. Lett.* **1997**, *33*, 143–147. (d) Zhang, Z. Z.; Sparks, D. L.; Scrivner, N. C. *Environ. Sci. Technol.* **1993**, *27*, 1625–1631.

10.1021/cm702206z CCC: $37.00
Published on Web 11/27/2007

mobilization of the reactive organic groups, preventing their leaching in the surrounding medium when the modified clay materials are to be used in solutions. The silylation of surfaces is well documented.[1,9] New prospects in various application areas have been opened by this approach, for example in catalysis and in separation technologies. The modification of the surface characteristics of silica or aluminosilicates is typically done by the reaction of silane derivatives such as chlorosilane, alkoxysilane, or organosilanes with silanol groups accessible on the surface.[10] In particular, aminoalkane-substituted silanes were amply used to modify silica and alumina surfaces[11] as well as periodic mesoporous silica.[12]

The chemical modification of 2:1 phyllosilicates by grafting with silanes occurs mainly on the hydroxyl groups of the external surface of the clay, i.e., by lateral interactions with the hydroxyl groups located on the edges of the clay particles.[8a,13] Coexistence of phases of interlayer grafted and externally grafted montmorillonite could be observed when the smectite is acidified before the grafting process.[14]

It is of interest to modify chemically the interlayer surfaces of layered materials since this operation could result in controlled nanohybrid two-dimensional architectures, suitable for specific catalytic reactions and controlled molecular separations. After intercalation by polar organic molecules, layered silicic acids such as magadiite were silylated by various organosilane reagents under dry conditions and reflux in an organic solvent[15] while the silylation of kenyaite was successfully done after gelification in the presence of octylamine and reaction at room temperature.[16] Kenyaite was also recently reacted with APTES and dodecylamine in ethanol, resulting in interlayer surface silylation.[17]

Kaolinite, of chemical formula $Al_2Si_2O_5(OH)_4$, is a dioctahedral 1:1 phyllosilicate formed by superposition of silicon tetrahedral sheets and aluminum octahedral sheets. It is characterized by two types of interlayer surfaces: a gibbsite-type surface covered by aluminol groups and a siloxane surface.[18] Adjacent layers are linked by van der Waals and H-bonds, which induce restricted access to the interlamellar aluminol groups that are however suitable candidates for grafting reactions. Taking into consideration this aspect, the covalent grafting of organosilane molecules onto the interlayer hydroxyl groups of the gibbsite side of kaolinite represents a synthetic challenge.

More recently, substantial efforts have been made to achieve the functionalization of kaolinite by organic groups after the intercalation in its structure of small polar molecules that increased the interlayer space and reduced the bond strength between consecutive layers. Thus, a range of compounds bearing hydroxyl groups were successfully grafted onto the internal OH groups of kaolinite.[19] So far, silylation reactions on kaolinite were reported to occur on the external surfaces of the particles.[20] Organosilane oligomers were shown to be adsorbed to the external surfaces of kaolinite by hydrogen bondings with no covalent bonds formed.[21] Reports on the silylation of aluminol groups are quite scarce. Johnson and Pinnavaia[22] have reported the reaction of the external Al–OH surfaces of imogolite with APTES under hydrolysis conditions.

The present work is focused on the preparation of a new class of organo-kaolinite nanohybrid materials, achieved by the interlayer grafting of a functionalized silane bearing amine groups. This was done by using kaolinite previously intercalated by DMSO or urea as precursors. Various physicochemical techniques were used to assess the efficiency of the grafting process.

(5) (a) Villemure, G.; Detellier, C.; Szabo, A. G. *Langmuir* **1991**, *7*, 1215–1222. (b) Ogawa, M. In *Handbook of Layered Materials*; Auerbach, S., Carrado, K. A., Dutta, P. K., Eds.; Marcel Dekker: New York, 2004;Chapter 5, pp 191–259. (c) Okada, T.; Ehara, Y.; Ogawa, M. *Chem. Lett.* **2006**, *35*, 638–639.
(6) (a) Nakatsuji, M.; Ishii, R.; Wang, Z. M.; Kenta, O. *J. Colloid Interface Sci.* **2004**, *272*, 158–166. (b) Wang, J. D.; Serrette, G.; Ying, T.; Abraham, C. *Appl. Clay Sci.* **1995**, *10*, 103–105.
(7) (a) Darder, M.; Colilla, M.; Ruiz-Hitzky, E. *Chem. Mater.* **2003**, *15*, 3774–3780. (b) Delozier, D. M.; Orwoll, R. A.; Cahoon, J. F.; Johnston, N. J.; Smith, J. G.; Connell, J. W. *Polymer* **2002**, *43*, 813–822.
(8) (a) Tonle, I. K.; Ngameni, E.; Njopwouo, D.; Carteret, C.; Walcarius, A. *Phys. Chem. Chem. Phys.* **2003**, *5*, 4951–4961. (b) Celis, R.; Hermosin, M. C.; Cornejo, J. *Environ. Sci. Technol.* **2000**, *34*, 4593–4599. (c) Ruiz-Hitzky, E.; Fripiat, J. J. *Clays Clay Miner.* **1976**, *24*, 25–30. (d) Hermosin, M. C.; Cornejo, J. *Clays Clay Miner.* **1986**, *34*, 591–596.
(9) Vansant, E. F.; van der Voort, P.; Vrancken, K. C. *Characterisation and Chemical Modification of the Silica Surface*; Elsevier: Amsterdam, The Netherlands, 1995.
(10) Impens, N. R. E. N.; van der Voort, P.; Vansant, E. F. *Microporous Mesoporous Mater.* **1999**, *28*, 217–232.
(11) Caravajal, G. S.; Leyden, D. E.; Quinting, G. R.; Maciel, G. E. *Anal. Chem.* **1988**, *60*, 1776–1786.
(12) (a) Harlick, P. J. E.; Sayari, A. *Ind. Eng. Chem. Res.* **2007**, *46*, 446–458. (b) Harlick, P. J. E.; Sayari, A. *Ind. Eng. Chem. Res.* **2006**, *45*, 3248–3255.
(13) (a) Maqueda, C. *Clays Clay Miner.* **1998**, *46*, 423–428. (b) Sheng, G.; Xu, S.; Boyd, S. A. *Soil Sci. Soc. Am. J.* **1999**, *63*, 73–78. (c) Alves, A. P. M.; Silva, A. L. P.; da Silva, O. G.; da Fonseca, M. G.; Arakaki, L. N. H.; Espinola, J. G. P. *J. Therm. Anal. Calorim.* **2007**, *3*, 771–774.
(14) Mercier, L.; Detellier, C. *Environ. Sci. Technol.* **1995**, *29*, 1318.
(15) (a) Ruiz-Hitzky, E.; Rojo, J. M. *Nature (London)* **1980**, *287*, 28–30. (b) Ruiz-Hitzky, E.; Rojo, J. M.; Lagaly, G. *Colloid Polym. Sci.* **1985**, *263*, 1025–1030.
(16) Thiesen, P. H.; Beneke, K.; Lagaly, G. *J. Mater. Chem.* **2002**, *12*, 3010–3015.
(17) Park, K.-W.; Jeong, S.-Y.; Kwon, O.-Y. *Appl. Clay Sci.* **2004**, *27*, 21–27.
(18) (a) Giese, R. F. In *Hydrous Phyllosilicates*; Bailey, S. W., Ed.; Mineralogical Society of America: Washington, DC, 1988; p 29. (b) Newman A. C. D.; Brown, G. In *Chemistry of Clays and Clay Minerals*; Newman A. C. D., Ed.; Longman Scientific and Technical, Mineralogical Society: London, 1987; Monograph No. 6, p 1.
(19) (a) Tunney, J. J.; Detellier, C. *Chem. Mater.* **1993**, *5*, 747–748. (b) Tunney, J. J.; Detellier, C. *Clays Clay Miner.* **1994**, *42*, 552–560. (c) Tunney, J. J.; Detellier, C. *J. Mater. Chem.* **1996**, *10*, 1679–1685. (d) Komori, Y.; Enoto, H.; Takenawa, R. J.; Hayashi, S.; Sugahara, Y. S.; Kuroda, K. *Langmuir* **2000**, *16*, 5506–5508. (e) Itagaki, T.; Kuroda, K. *J. Mater. Chem.* **2003**, *13*, 1064–1068. (f) Brandt, K. B.; Elbokl, T. A.; Detellier, C. *J. Mater. Chem.* **2003**, *13*, 2566–2572. (g) Murakami, J.; Itagaki, T.; Kuroda, K. *Solid State Ionics* **2004**, *172*, 279–282. (h) Gardolinski, J. E. F. C.; Lagaly, G. *Clay Miner.* **2005**, *40*, 537–546. (i) Gardolinski, J. E. F. C.; Lagaly, G. *Clay Miner.* **2005**, *40*, 547–556. (j) Elbokl, T. A.; Detellier, C. *Clay Sci., Suppl. 1* **2005**, *12*, 38–46. (k) Janek, M.; Emmerich, K.; Heissler, S.; Nüesch, R. *Chem. Mater.* **2007**, *19*, 684–693. (l) Letaief, S.; Detellier, C. *Chem. Commun.* **2007**, 2613–2615.
(20) (a) Braggs, B.; Fornasiero, D.; Ralston, J.; Smart, R. St. *Clays Clay Miner* **1994**, *42*, 123–136. (b) Zhang, Y.; Gittins, D. I.; Skuse, D.; Cosgrove, T.; van Duijneveldt, J. S. *Langmuir* **2007**, *23*, 3424–3431. (c) Porro, T. J.; Pattacini, S. C. *Appl. Spectrosc.* **1990**, *44*, 1170–1175.
(21) Johansson, U.; Holmgren, A.; Forsling, W.; Frost, R. L. *Clay Miner.* **1999**, *34*, 239–246.
(22) (a) Johnson, L. M.; Pinnavaia, T. J. *Langmuir* **1990**, *6*, 307–311. (b) Johnson, L. M.; Pinnavaia, T. J. *Langmuir* **1991**, *7*, 2636–2641.

The modified clays were evaluated as electrode modifiers by a strategy based on the protonation of amine groups of the grafted clays. To that effect, the organoclays were coated on the surface of a platinum electrode and used in 0.1 mol L^{-1} KCl acidified by HCl to pH 3 for the electrochemical preconcentration leaching of $[Ru(CN)_6]^{4-}$ anions through multisweep cyclic voltammetry.

Experimental Section

Starting Materials and Preparation of the Precursors. Two clays were used in this study: a well-crystallized kaolinite (KGa-1b, denoted hereafter as K) obtained from the Source Clays Repository of the Clay minerals Society (Purdue University, West Lafayette, IN) and a cameroonian kaolinite (sample MY45S, denoted hereafter as M) collected from Mayouom kaolin deposit (Noun division, Western Cameroon) fully characterized by Njoya et al.[23] Both samples were purified according to standard sedimentation techniques, and the experiments were conducted on the <2 μm clay fraction.

The intercalation of DMSO and urea in the interlayer space of the purified clays was done according to previously published procedures.[24] Briefly, 10 g of the clay fraction was suspended in 50 mL of DMSO (Fisher Scientific), and the mixture was stirred at 80 °C in an enclosed jar, using a magnetic stirrer. The intercalation reaction was daily monitored by analyzing XRD patterns of the clay complex smeared onto a glass slide and comparing the peak intensities of the intercalated vs nonintercalated d_{001} values. After 7 days, the clay–DMSO complex was washed with 1,4-dioxane (99.9%, Fisher Scientific) to remove excess DMSO. After air-drying for 12 h, the product was gently ground in a mortar. The DMSO-intercalated intermediates were designed by KD and MD respectively for K and M purified clays. The intercalation of kaolinite with urea was accomplished by dry milling: a mixture formed by 4 g of urea (Aldrich) and 3 g of the clay material was mechanically milled at room temperature, the extent of intercalation being regularly monitored by the intercalation ratio using XRD powder analysis.[24b] Upon complete intercalation, the resulting material (KU or MU respectively for K and M samples) was washed two times with 30 mL of isopropanol and dried at 90 °C for 1 h.

Aminosilane Grafting Process. The procedure used for the synthesis of the organoclay is described as follows: 1 g of KD (or MD), previously dried by heating at 90 °C for 30 min, was placed in a 25 mL flask; under stirring, 5 mL of APTES (99%, Sigma-Aldrich) was slowly added by the means of a syringe under a dried nitrogen atmosphere. The mixture was heated at 195 °C for 48 h under nitrogen. After cooling, the product was filtered and washed several times with a total amount of 30 mL of toluene (99%, Fisher Scientific) to remove unreacted APTES and then dried in vacuum at 110 °C for 14 h. The resulting material was ground in a mortar and kept in a plastic tube for further characterization and utilization. Throughout the text, the APTES-functionalized derivatives are noted KDN and MDN respectively for KD and MD precursors. Identical procedures were followed in the case of KU and MU, and the final materials were designed as KUN and MUN.

Instrumentation and Analytical Procedures. The starting purified clay minerals (K, M), their DMSO intercalation precursors (KD, MD), and the final nanohybrid materials (KDN, MDN, KUN, and MUN) were characterized by X-ray diffraction (XRD), Fourier transform infrared (FTIR) spectrometry, solid-state nuclear magnetic resonance (NMR), and thermogravimetric analysis.

XRD patterns were obtained on a Philips PW 3710 Instrument equipped with Ni filter and Cu Kα radiation ($\lambda = 1.540\,56$ Å) using a generator voltage of 45 kV and a generator current of 40 mA.

Infrared spectra were acquired between 4000 and 400 cm^{-1} on an ABB Bomem FTIR instrument under dry air. The resolution was kept at 4 cm^{-1}, and the number of scans was 24. The spectra were measured using KBr pellets (sample mass fraction <0.05 in KBr). All the displayed spectra were recorded at room temperature after thermal pretreatment in an oven at 100 °C for 30 min to evacuate most of the physically sorbed water.

A simultaneous thermal analysis (STA) device (model SDT 2960, TA Instruments) linked to a quadrupole mass spectrometer (QMS 422) allowed simultaneous collection of signals relative to mass loss, heat flow, and evolved gases during heating. Approximately 10–20 mg of the clay material was placed on the thermobalance of the STA analyzer, which was purged with helium gas. The measurements were recorded from room temperature to 1100 °C with a temperature ramp of 10 °C min^{-1}, and data analysis was performed using Universal Analysis 2000 software package. The results are expressed by the thermal gravimetric (TG) weight loss curve and by the first derivative of this curve, i.e., the differential thermal gravimetric (DTG) curve.

The ^{13}C NMR data were collected under quantitative conditions on a Bruker AVANCE 500 NMR spectrometer. 50 mg of sample was packed in a 4 mm zirconia rotor and spun at 12 kHz at the magic angle. The sample was run using a simple block decay sequence with 90° ^{13}C pulses and high-power proton decoupling. The 90° pulse was 2.88 μs, and the decoupling power was 70 kHz. A total of 7767 scans were collected using a recycle delay of 60 s and an acquisition time of 25 ms. The total data collection time was greater than 5 days. The NMR spectrum had a very broad background signal with a width at half-height of ~150 ppm centered at ~120 ppm from the kel-F rotor cap and, to a lesser extent, other plastic parts near the coil of the NMR probe. In order to obtain a flat baseline for integration, the baseline was corrected only in the range of 200 to −10 ppm using the software of the spectrometer. There was no appreciable spinning sideband intensity so no corrections were made for it.

The ^{13}C NMR spectrum of pure APTES was collected on a Bruker AVANCE 400 NMR spectrometer operating at 100.67 MHz for ^{13}C. Approximately 0.5 mL of the sample was dissolved in ~2 mL of $CDCl_3$ in a 5 mm NMR tube. A simple one-pulse experiment was employed with continuous proton decoupling using the WALTZ 16 sequence. 30° ^{13}C pulses were used with a 1 s acquisition time and a 1 s recycle delay. The spectral width was set at 24 038 Hz, and 51 200 data points were collected for each free induction decay. The data collection time was 5 min. The ^{13}C chemical shifts were referenced to TMS at 0 ppm using the signal of $CDCl_3$ at 77 ppm as a secondary standard.

^{29}Si MAS spectra were collected on a Bruker ASX 200 NMR spectrometer operating at 39.75 MHz for ^{29}Si. Approximately 300 mg of sample was packed in a 7 mm o.d. zirconia rotor which was spun at the magic angle at 4 kHz. A simple Block decay experiment was employed with a 4.25 μs ^{29}Si pulse (90°) and a 58 kHz CW proton decoupling field during the 50 ms acquisition time. The recycle delay was 5 s. The spectral width was set at 10 060 Hz, and 1K data points were collected for each of 47 606 free induction decays. The data collection time was 66 h. The ^{29}Si chemical shifts were referenced to TMS at 0 ppm using the high-frequency signal of tetrakis(trimethylsilyl)silane at −9.9 ppm as a secondary standard.

(23) Njoya, A. A.; Nkombou, C.; Grosbois, C.; Njopwouo, D.; Njoya, D.; Nomade, A. C.; Yvon, J.; Martin, F. *Appl. Clay Sci.* **2006**, *32*, 125–140.

(24) (a) Letaief, S.; Detellier, C. *J. Mater. Chem.* **2005**, *15*, 4734–4740. (b) Letaief, S.; Elbokl, T. A.; Detellier, C. *J. Colloid Interface Sci.* **2006**, *302*, 254–258. (c) Letaief, S.; Detellier, C. *J. Mater. Chem.* **2007**, *17*, 1476–1484.

Electrochemical Procedures, Instrumentation, and Reagents. For the preparation of the clay-modified electrodes, 8 mg of the clay material (raw or modified kaolinite) were added to 5 mL of a 10 wt % dispersion in water of polystyrene (Aldrich) and agitated for 10 min. 1 mL of the obtained suspension was spin-coated at 500 rpm for 10 min onto a platinum electrode (approximate surface area: 0.20 cm^2) held in the inverted position on an analytical rotator (Caframo, type RZR 50). The resulting clay-modified electrode was allowed to dry at room temperature for 90 min and used for electrochemical measurements without any other treatment. Prior to the film deposition, the platinum electrode was polished using 0.05 μm alumina (CH Instruments) and rinsed with copious amounts of water to remove any remaining alumina.

Multisweep cyclic voltammetry (MCV) experiments were conducted using an instrumentation based on a potentiostat/galvanostat (model HA-303, HD) and a Nicolet 310 digital oscilloscope coupled with an Hokuto Denko HB-104 function generator capable of applying linear potential scans to the potentiostat. The data from current–potential curves recorded on the Nicolet 310 digital oscilloscope were stored on floppy diskettes and then transferred to a computer for further processing. Measurements were performed in a three-electrode cell comprising either the bare platinum or the clay film-modified platinum working electrode, a platinum wire auxiliary electrode (Metrohm, ref 6.0301.100), and an Ag/AgCl reference (Metrohm, ref 6.0726.100). All experiments were run at room temperature, from −0.5 to +0.3 V at a scan rate of 100 mV s^{-1}.

$K_4Ru(CN)_6 \cdot 3H_2O$ (Alfa) and KCl (Aldrich) were reagent grade and used as received. HCl (36%) was obtained from Merck.

Results and Discussion

Silylation reactions using 3-aminopropyltriethoxysilane (APTES) have been conducted so far in a variety of conditions. The solvents used ranged from water[22,25] or aqueous–organic mixtures[26] to ethanol in the presence of an alkylamine[17,27] and to dry toluene.[8a,11,28] APTES was also deposited on silica from the gas phase.[29]

The silylation of kaolinite by APTES was attempted on two samples of kaolinite: a highly crystalline one, KGa-1b (K), and a poorly crystalline one from Cameroon, MY45S (M). In both cases, the reaction of kaolinite (K and M) and of kaolinite preintercalated with DMSO (KD and MD) or urea (KU and MU) with APTES was attempted under a variety of conditions, using dry toluene under reflux for 24 h either under dry nitrogen or under air. The reactions performed under air resulted in kaolinite particles distributed in a polymeric organosilane matrix without intercalation, the DMSO intercalate being displaced during the process. Under dry nitrogen, the kaolinite particles were also recovered without intercalation as shown by the XRD data. Kaolinite samples intercalated by urea behaved according to the same trend, and the resulting materials were not further characterized since the goal of the experiments was the interlayer grafting on the aluminol surface. The strategy used for this goal was based on the previous successful kaolinite intercalation of ionic liquids[24] and of poly(ethylene glycol)[30] consisting in taking advantage of a concentration effect by using the compound to be intercalated as the solvent. Consequently, previously dried K, M, KD, and MD were stirred under dry nitrogen in APTES at 195 °C for 48 h, a temperature slightly below its boiling point. No intercalation could be observed in the cases of K and M. However, in both KD and MD, a d_{001} diffraction peak was observed at 1.64 nm, indicating intercalation. The resulting material is noted KDN or MDN, for amino-functionalized silylated kaolinite.

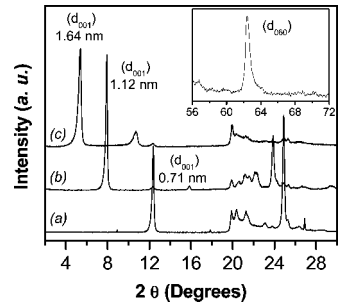

Figure 1. X-ray powder diffraction patterns of (a) K, (b) KD, and (c) KDN. Inset: XRD pattern of KDN showing the d_{060} reflection of kaolinite.

Figure 1 gives the X-ray powder diffraction pattern of oriented samples of K, KD, and KDN. The 1.12 nm d_{001} peak characteristic of kaolinite intercalated by DMSO has been fully replaced after reaction with APTES by a new peak at 1.64 nm, corresponding to an interlayer distance of 0.93 nm. The distance of 1.64 nm is larger than what is commonly observed in intercalated or grafted kaolinite materials, typically in the range 0.9–1.2 nm,[19,31] indicating either the presence of larger molecular species arranged in a nonflattened configuration or the formation of a bilayer.

Large basal spacings, up to 6.42 nm, have been reported for the intercalation of long chain alkyl amines in kaolinite.[19i,32] The d_{060} reflection of kaolinite remains at 62.5° 2θ (1.49 Å), characteristic of a dioctahedral clay mineral and showing that the structure of the kaolinite layers is largely unaffected in the *a,b* plane by the reaction process. The intercalation ratio is more than 95%, as indicated, as a first approximation, by the relative intensities of the d_{001} diffraction peaks of intercalated and unintercalated kaolinite respectively at 1.64 and 0.71 nm. Similar results were obtained in the case of the M kaolinite, with broader diffraction peaks due to poorer crystallinity.

The FTIR spectra of the two kaolinite samples, their DMSO intercalates, and their APTES grafted materials are

(25) (a) Bourlinos, A. B.; Jiang, D. D.; Giannelis, E. P. *Chem. Mater.* **2004**, *16*, 2404–2410. (b) Nakao, T.; Nogami, M. *Mater. Lett.* **2005**, *59*, 3221–3225.

(26) (a) Szabó, A.; Gournis, D.; Karakassides, M. A.; Petridis, D. *Chem. Mater.* **1998**, *10*, 639–645. (b) Ahenach, J.; Cool, P.; Impens, R. E. N.; Vansant, E. F. *J. Porous Mater.* **2000**, *7*, 475–481. (c) He, H. P.; Duchet, J.; Galy, J.; Gerard, J. F. *J. Colloid Interface Sci.* **2005**, *288*, 171–176. (d) Shanmugharaj, A. M.; Rhee, K. Y.; Ryu, S. H. *J. Colloid Interface Sci.* **2006**, *298*, 854–859. (e) Chujo, T.; Gonda, Y.; Oumi, Y.; Sano, T.; Yoshitake, H. *J. Mater. Chem.* **2007**, *17*, 1372–1380.

(27) Park, K.-W.; Kwon, O.-Y. *Bull. Korean Chem. Soc.* **2004**, *25*, 965–968.

(28) (a) Mukkanti, K.; Subba Rao, Y. V.; Choudary, B. M. *Tetrahedron Lett.* **1989**, *30*, 251–252. (b) Tonle, I. K.; Ngameni, E.; Walcarius, A. *Electrochim. Acta* **2004**, *49*, 3435–3443. (c) Matsuo, Y.; Nishino, Y.; Fukutsuka, T.; Sugie, Y. *Carbon* **2007**, *45*, 1384–1390.

(29) (a) Ek, S.; Iiskola, E. I.; Niinistö, L.; Pakkanen, T. T.; Root, A. *Chem. Commun.* **2003**, *2032]?>*, 2033. (b) Ek, S.; Iiskola, E. I.; Niinistö, L.; Vaittinen, J.; Pakkanen, T. T.; Root, A. *J. Phys. Chem. B* **2004**, *108*, 11454–11463.

(30) Tunney, J. J.; Detellier, C. *Chem. Mater.* **1996**, *8*, 927–935.

(31) Tunney, J. J.; Detellier, C. *Can. J. Chem.* **1997**, *75*, 1766–1772.

(32) Komori, Y.; Sugahara, Y.; Kuroda, K. *Appl. Clay Sci.* **1999**, *15*, 241–252.

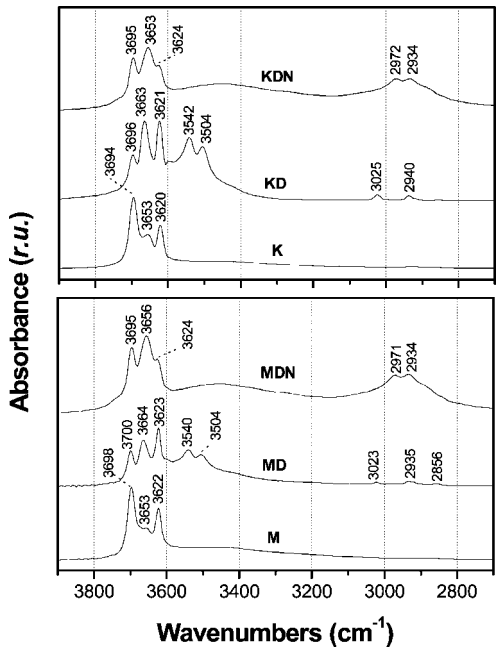

Figure 2. IR spectra (3900–2700 cm^{-1}) of pure clay materials (K, M), their DMSO intercalation compounds (KD, MD), and their APTES grafted derivatives (KDN, MDN).

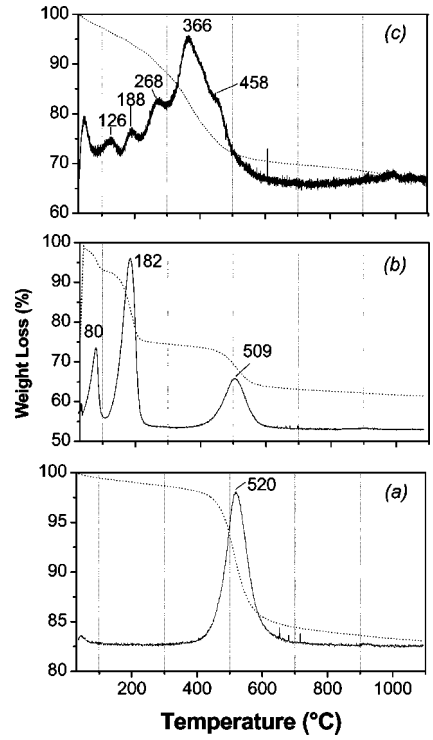

Figure 3. TG (dotted line) and DTG (solid line) curves (RT–1100 °C) of (a) K, (b) KD, and (c) KDN.

given in Figure 2 for the region 2700–3900 cm^{-1}. The two series of spectra are almost identical for the two kaolinite samples, indicating the same reactivity response toward the thermal treatment with APTES. The OH stretching region of kaolinite is sensitive to the effects of interlayer modification, and the intercalation and grafting of the organosilane on the aluminol internal surface should have a major influence on the OH stretching pattern of kaolinite. This is indeed observed in Figure 2, where the IR pattern of KDN is very different from that of the parent kaolinite material or of the preintercalate with DMSO. The internal OH stretching vibration at 3620 cm^{-1} is still observed as a shoulder at 3624 cm^{-1}, confirming that the reaction with APTES did not modify the 1:1 layer structure of kaolinite.

The band observed in the range 3694–3700 cm^{-1} in all the samples is attributed to the stretching of the interlayer hydroxyl groups pointing almost perpendicularly to the *c*-direction. They are not expected to be involved in H-bonding with intercalates or in a grafting reaction. In contrast, a band appears at 3653 cm^{-1} which is attributed to unreacted inner-surface hydroxyl groups interacting with the organosilane. This is similar to what was observed previously in cases of various grafted alkoxy groups.[19c,h] The stretching vibrations bands of the organosilane C–H groups are observed at 2972 and 2934 cm^{-1}.

Figure 3 shows the TGA and DTG traces of K, KD, and KDN under nitrogen flow. The dehydroxylation peak of kaolinite observed at 520 °C is moved to a lower temperature, 509 °C in the case of the DMSO intercalate. The loss of DMSO at 182 °C is in a temperature range typical of an intercalate, as was observed, for example, for ethanolamine at 198 °C[19l,31] or for ethylene glycol at 168 °C.[19k] The thermal traces in the case of KDN are very different. A continuous multistep mass loss is observed from approximately 120 to 500 °C. This more complicated thermal behavior is diagnostic of grafted species decomposing at various temperatures. The dehydroxylation of kaolinite is no longer observed in its typical temperature range. A shoulder on the DTG trace observed at 458 °C can be attributed to the dehydroxylation of the aluminol groups not involved in the grafting process. These observations are similar to what was previously reported for other grafted species on the interlayer surfaces of kaolinite, in the case ot triethanolamine[19l] or glycerol[19k] for example. The ionic intensity curves of molecular fragments were recorded for a series of masses under He flow. The peaks at 126 and 188 °C on the DTG trace correspond principally to the fragment $m = 44$ g mol^{-1}, attributed to $C_2H_4O^+$ resulting from the decomposition of the organosilane ethoxy groups. A molar mass of 18 g mol^{-1} was detected at 442 °C and attributed to the dehydroxylation of the kaolinite layers. The largest mass loss, observed around 366 °C on the DTG trace, corresponds to a variety of heavier fragments at 39, 40, and 42 g mol^{-1}. These are typical of nitrogen-containing fragments, such as C_2HN^+, $C_2H_2N^+$, $C_2H_4N^+$, or $C_3H_6^+$. The fragment at 44 g mol^{-1} is again observed at 350 °C.

The thermal behavior of the cameroonian kaolinite, M, is very similar, with dehydroxylation observed at 507 and 505 °C respectively for M and MD, and a complex, multistep, weight loss for MDN, corresponding very closely to the KDN case described above.

The ^{13}C MAS NMR spectrum of the organosilane kaolinite derivative is given in Figure 4. The conditions of the spectrum were carefully chosen to obtain quantitative data (see Experimental Section). For comparison, the high-resolution ^{13}C NMR spectrum of APTES was recorded in $CDCl_3$. It is given also in Figure 4.

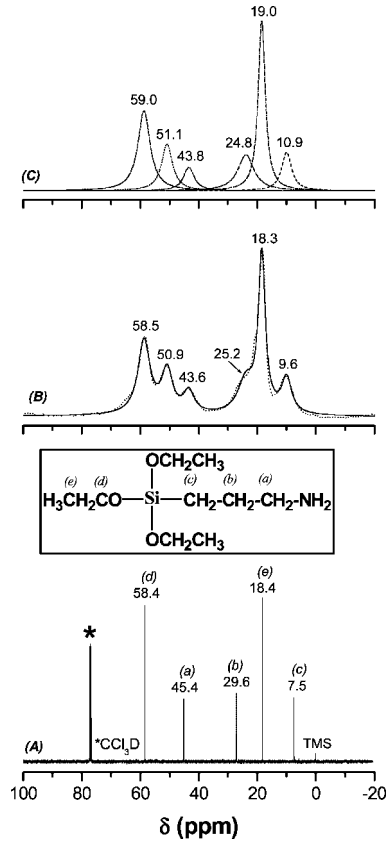

Figure 4. ^{13}C NMR spectra of (A) pure APTES, (B) KDN (dotted line for experimental and solid line for simulated), and (C) deconvolution results of the experimental spectrum. The spectrum of pure APTES was recorded in solution, whereas that of KDN was recorded in the solid state.

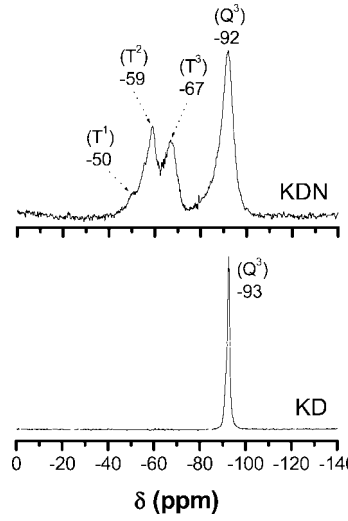

Figure 5. Solid-state ^{29}Si CP-MAS spectra of KD and KDN.

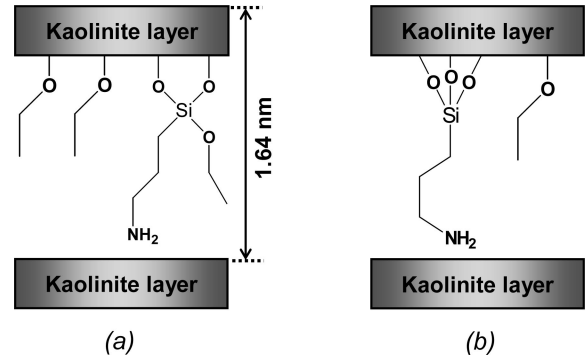

Figure 6. Schematic representation showing the structural possibilities of the grafting of organosilyl and ethoxy groups on the kaolinite interlayer space.

One can observe six signals for the nanohybrid material, the minor signal at 43.6 ppm being attributed to residual DMSO molecules and the other five signals to the ethoxy and propyl signals originating from APTES. The two signals of the ethoxy groups at 58.5 and 18.3 ppm (as observed before deconvolution) remain the preponderant ones.

Figure 4c gives the result of the deconvolution of the signals. The residual DMSO accounts for 6.5% of the total intensities. The three signals corresponding to the propyl group have an integration of 9.8, 14.7, and 13.2% respectively for the 10.9, 24.9, and 51.1 ppm signals, for an average of 12.6%. The two signals corresponding to the ethoxy groups are integrated for 30.8 and 25.0% respectively for the 19.0 and 59.0 ppm signals, for an average of 27.9%. The percentage ratio of one ethoxy carbon over one propyl carbon is 2.2 to be compared with 3.0 in the original APTES molecule, before reaction with kaolinite. The ^{13}C CP/MAS NMR spectrum of the MDN material gave similar qualitative results with the five peaks of the ethoxy and propyl groups at approximately the same chemical shift, with some residual DMSO.

The ^{29}Si CP/MAS NMR spectra of KD and KDN are shown in Figure 5. One Q^3 signal is observed at −93.1 ppm for KD, with a minor shoulder at −91.0 ppm, corresponding to the minor amount of unexpanded kaolinite.[24c]

On the basis of the ^{29}Si NMR data, showing an almost complete bidentate or tridentate fixation of APTES on kaolinite, one would expect that a very large fraction of the ethoxy groups should be evacuated as ethanol. However, this is in apparent contradiction with the ^{13}C NMR data, since the percentage ratio of ethoxy groups over propyl groups is still 2.2.

This apparent contradiction can be resolved if one compares the reaction conditions with those used previously for the grafting of methoxy groups on the internal layers of kaolinite.[19c] Under similar temperature conditions, in the range 180–200 °C, the interlayer surface of kaolinite was methoxylated by the reaction of methanol with the aluminol surface. Consequently, it is highly plausible that, once generated by the silanation reaction, ethanol reacts with neighboring aluminol groups to produce a nanohybrid material with two types of grafted moieties: 3-aminopropylsilyl and ethoxy groups, in an approximate ratio of 1:2 (Figure 6).

This structure is corroborated by the results of the CHN elemental analysis of KDN and MDN. The case of KDN will be described here. The results are similar for MDN. The elemental analysis of KDN gives C: 13.11%; H: 3.55%; and N: 2.02%, in good agreement with the TGA data. Taking as a working hypothesis the reactions schematized in Figure 6, neglecting the contribution of the T^1 groups, and considering that two aluminol groups are available for grafting by kaolinite structural units, a structural model involving two kaolinite structural units is proposed, in which either the

grafting is bidentate (Figure 6a) with a concurrent grafting of the two ethoxy groups generated by the silylation reaction or the grafting is tridentate (Figure 6b) with the concurrent grafting of one ethoxy group and the loss of two ethanol molecules.

Consequently, under this hypothesis, the chemical formula of the resulting nanohybrid material becomes $Al_4Si_5O_{18}H_xN_yC_z$. From the results of the CHN analysis, resolving the three equations with three unknowns gives $x = 23.2$, $y = 0.95$, and $z = 7.2$ or the formula $Al_4Si_5O_{18}H_{23.2}N_{0.95}C_{7.2}$. Under this model, the chemical formula would be $Al_4Si_5O_{18}H_{27}NC_9$ and $Al_4Si_5O_{18}H_{17}NC_5$ respectively for a bidentate and a tridentate fixation. The experimental results are midway between these two formula, suggesting an approximate ratio 1:1 for the distribution of bidentate and tridentate species, in excellent agreement with the ^{29}Si NMR data and with the ^{13}C NMR data since, under a 1:1 distribution, the expected ethoxy:propyl ratio is 2, very close to the experimental ^{13}C quantitative results of 2.2.

The material is resistant to a certain extent to hydrolysis. When KDN was washed for 2 h with water, no detectable changes were observed on the XRD pattern. After 24 h of water washing, the phase at 1.6 nm was still present but together with another phase at 1.0 nm. Plausibly the Al–O–Si bond is partially hydrolyzed, as it was observed previously in the case of imogolite,[22] while the Al–O–C resists under these conditions.[19] Interestingly, the observation of two different phases indicated a synergistic effect in the hydrolysis process, which is plausibly done layer by layer.

In order to explore the possible use of the amino-functionalized kaolinite materials as electrode modifiers, some preliminary experiments were performed for electroanalysis of $[Ru(CN)_6]^{4-}$ species chosen as electroactive probe. Since the organokaolinites bear aminopropyl groups, it is expected that positive charges could be created by a simple protonation on the basis of the acid–base properties of the alkylamine moieties, that is, by working in acidic medium in which the organoclay may be maintained in the protonated form. In such conditions, the internal surface properties may be turned from neutral to positive, bringing anion exchange properties to the functionalized material. However, highly concentrated acidic media (pH < 2) are to be excluded for the investigations, to avoid the possible degradation of the clay sheets that occurs in strongly acidic medium due to the acid hydrolysis of Al centers.[33] Thus, a solution of 0.1 M KCl acidified to pH 3 by diluted HNO_3 was chosen as supporting electrolyte for electrochemical experiments.

The electrochemical behavior of $[Ru(CN)_6]^{4-}$ was first examined in the supporting electrolyte at the bare platinum electrode. Figure 7a depicts the signal obtained for a solution containing 1 mM $[Ru(CN)_6]^{4-}$ anions: cyclic potential scanning between −0.5 and +0.3 V exhibits an electrochemical response at $Ep_a = -0.10$ V in the oxidation direction and $Ep_c = -0.21$ V in the cathodic direction. This

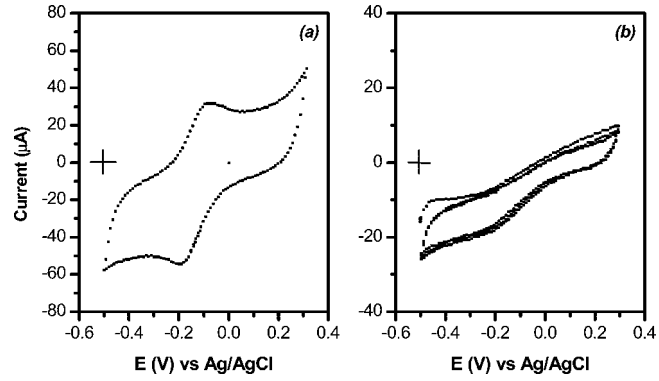

Figure 7. Multisweep cyclic voltammograms recorded in 10^{-3} mol L^{-1} $[Ru(CN)_6]^{4-}$ (supporting electrolyte: 0.1 mol L^{-1} KCl at pH 3) using (a) an unmodified platinum electrode and (b) the platinum electrode modified by spin-coating of purified kaolinite. Potential scan rate: 100 mV s^{-1}.

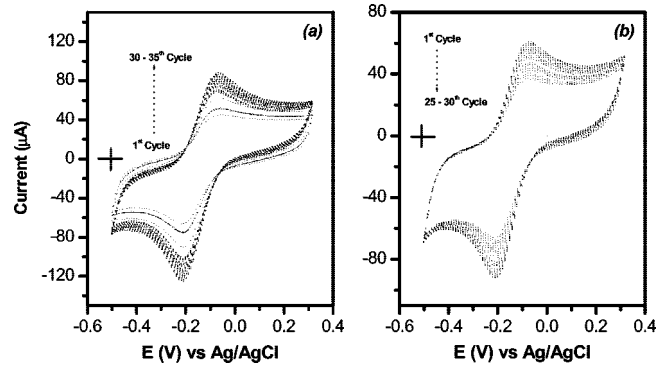

Figure 8. Multisweep cyclic voltammograms recorded (a) in 10^{-3} mol L^{-1} $[Ru(CN)_6]^{4-}$ (supporting electrolyte: 0.1 mol L^{-1} KCl at pH 3) using KDN clay film coated on platinum eletrode and (b) after upon saturation, the electrode was transferred in the supporting electrolyte free from $[Ru(CN)_6]^{4-}$ anions. Potential scan rate: 100 mV s^{-1}.

leads to $E_{1/2} = -0.16$ V (vs Ag/AgCl), corresponding to the oxidation–reduction of the $[Ru(CN)_6]^{4-}/[Ru(CN)_6]^{3-}$ couple.

Upon continuous cycling, this voltammogram was quite stable, the ratio of the anodic peak current (Ip_a) and the cathodic peak current (Ip_c) measured from the extrapolated baseline being equal to 1.

When the bare platinum electrode was modified by spin-coating with a film of purified kaolinite, continuous cycling in the same conditions as in Figure 7a gave a flat voltammogram (Figure 7b), implying that $[Ru(CN)_6]^{4-}$ anions were not retained by the clay film at the electrode.

The lack of any electrochemical response in that case can be fully interpreted by the fact that both the tetrahedral siloxane surface and the octahedral basal surface (gibbsite sheet) of kaolinite are electrically neutral. The film coated on the electrode hence acts as a physical barrier, preventing the access to the active surface of the platinum by the $[Ru(CN)_6]^{4-}$ analyte.

The propylammoniumsilane-modified kaolinite nanohybrid materials, coated on the platinum electrode surface, were applied in ion exchange voltammetry using the same $[Ru(CN)_6]^{4-}$ electroactive probe as in the case of the raw kaolinite-modified electrodes. Figure 8a shows that the presence of the modified kaolinite film at the platinum surface electrode enhances sensitively in its voltammetric response toward the $[Ru(CN)_6]^{4-}$ anions. This is matched

(33) (a) Manisankar, P.; Gomathi, A. *Bull. Chem. Soc. Jpn.* **2005**, *78*, 1783–1790. (b) Jozefaciuk, G.; Szatanik-Kloc, A.; Shin, J.-S. *Environ. Sci. Res.* **1998**, *55*, 329–335.

by the progressive accumulation of the negatively charged electroactive probe by an anion exchange with Cl^- anions from the electrolyte in the bulk of the clay film. The protonated modified clay of the film acts presently as a very efficient anion collector, giving rise after about 32 cyclic scans to a steady-state voltammogram. The peak current values obtained upon saturation of the film are $Ip_a = 83\ \mu A$ (anodic) and $Ip_c = 98\ \mu A$ (cathodic), corresponding to more than 3.8 and 4.4 times the values obtained at the bare electrode respectively in the anodic and cathodic directions.

It is important to mention that during the preconcentration of $[Ru(CN)_6]^{4-}$ by the organokaolinite materials the peak height for the reduction wave was higher than that of the anodic wave for each cyclic voltammogram. The ratio between Ip_a and Ip_c at saturation was 0.85, whereas the value of the same parameter was equal to 1 at the unmodified platinum electrode. This trend is probably related to the difference in the diffusion or to the speed of mass transfer for the probe within the film on platinum, as these factors are likely to affect the behavior of redox species at clay-modified electrodes. In the electrochemical section of this work, we were interested by the development of a selective surface for the entrapment of electroactive anionic species. Further investigations will be devoted to an examination of the parameters that can affect and govern the diffusion of $[Ru(CN)_6]^{4-}$ in the clay film electrodes obtained from the materials herein prepared.

The progressive accumulation of $[Ru(CN)_6]^{4-}$ species through multisweep potential scanning is typical of what is usually observed for anions trapping at clay modified electrodes.[34] The same trend was observed either with KDN or MDN film electrodes, in agreement with previous report dealing with $[Fe(CN)_6]^{3-}$, a similar probe examined at a smectite-type clay also functionalized by APTES and coated on a glassy carbon electrode.[35]

Finally, when the $[Ru(CN)_6]^{4-}$ exchanged film obtained upon saturation was rinsed with water and transferred to a solution containing only the supporting electrolyte (free from $[Ru(CN)_6]^{4-}$), the peak current was found to decrease continuously upon multisweep potential scanning (Figure 8b). A reverse ion exchange of $[Ru(CN)_6]^{4-}$ for the electrolyte anions (Cl^-) is the phenomenon involved. These electrochemical results are an additional indication that the grafting process of APTES on the interlayer spaces of kaolinite was quite effective.

In conclusion, a new type of nanohybrid material was prepared from the abundant clay mineral kaolinite. A kaolinite DMSO or urea preintercalate was reacted in the absence of any other molecules, such as a solvent, in dry conditions, with 3-aminopropyltriethoxysilane at a temperature slightly below its boiling point. All the experimental data, particularly TGA/MS and ^{29}Si MAS NMR data, joined to the observed resistance of the material to hydrolysis, point to the concomitant silylation and ethoxylation of the interlayer aluminol surface to afford a mixed alkoxy–organosilyl kaolinite derivative. The silylation was roughly equally distributed between bidentate and tridentate fixations, with a minor amount of monodentate material. The modified kaolinite materials were relatively resistant to hydrolysis, allowing their possible exploitation as electrode modifiers through clay film electrodes. Once spin-coated on a platinum substrate, these materials showed the ability to ion exchange ruthenium hexacyanide species in acidic media that promote their protonation, thus bringing anion exchange properties to kaolinite.

Acknowledgment. This work was financially supported by a Discovery Grant of the Natural Sciences and Engineering Research Council of Canada (NSERC) and the International Foundation for Science (grant W/3908-1). L'Agence Universitaire de la Francophonie (AUF) is thanked for a postdoctoral fellowship to Dr. Tonle. Dr. Glenn A. Facey is thanked for recording the NMR spectra and setting up their experimental conditions.

CM702206Z

(34) (a) Stein, J. A.; Fitch, A. *Clays Clay Miner.* **1996**, *44*, 381–392. (b) Navratilova, Z.; Kula, P. *Electroanalysis* **2003**, *15*, 837–846.

(35) Ngameni, E.; Tonle, I. K.; Apohkeng, J. T.; Bouwe, R. G. B.; Jieumboue, A. T.; Walcarius, A. *Electroanalysis* **2006**, *18*, 2243–2250.